3D Dynamic Finite Element Model for Magnetostrictive Galfenol-based Devices

Suryarghya Chakrabarti, Marcelo J. Dapino

The Ohio State University, Columbus, OH, USA, 43210

ABSTRACT

Galfenol is an alloy of iron and gallium which possesses a unique combination of structural strength and significant magnetostriction. This alloy can be machined, welded and extruded into complex geometries opening up avenues for a new class of load-bearing transducers with 3D functionality. This work addresses the development of an advanced modeling tool to aid in the design of Galfenol transducers. The model describes the full nonlinear coupling between the electrical, magnetic and mechanical domains in 3D Galfenol structures, yielding complete system input-output relationships. Maxwell's equations for electromagnetics and Navier's equations for mechanical systems are formulated in weak form. An energy-averaged constitutive model is employed to relate magnetization and strain to magnetic field and stress in the Galfenol domain. The overall system is approximated hierarchically; first, piecewise linearization is used to describe quasi-static responses and magnetic bias calculations. A linear dynamic solution with piezomagnetic coefficients computed at the bias point describes the system dynamics for moderate inputs. Dynamic responses at large input fields and stresses are described through an implicit dynamic solution based on the trapezoidal rule. The model equations are solved on a commercial finite element solver. A case study consisting of a Galfenol unimorph is presented which illustrates the model's ability to describe transient dynamic responses.

Keywords: Galfenol, finite element modeling, unimorph actuator, magnetostrictive materials

1. INTRODUCTION

Magnetostrictive iron-gallium alloys (Galfenol) possess structural-grade mechanical properties in addition to exhibiting moderate magnetostriction. These properties make Galfenol uniquely well-suited for integration within three-dimensional (3D) active structures. Galfenol can be used in sensors or actuators capable of withstanding tension, compression and shock loads. To design Galfenol structures, a modeling framework is required for describing the full nonlinear coupling between the electrical, magnetic and mechanical domains. A Galfenol system consists of a Galfenol driver (possibly with complex 3D geometry), passive magnetic materials for flux completion, passive structural materials for load transmission, permanent magnetic materials for magnetic biasing, and copper coils for generation of dynamic fields. Depending on whether the Galfenol driver is used as a sensor or actuator, the inputs and outputs consist of various combinations of the magnetic conjugate variables (magnetic field and magnetic induction) with the mechanical conjugate variables (strain and stress).

Significant effort has been concentrated on developing coupled models for magnetostrictive transducers. In particular, attention has been paid to 1D transducers with Terfenol-D loaded unidirectionally. Dapino et al.[1] coupled the Jiles-Atherton model with a wave equation describing the structural dynamics of a Terfenol-D actuator. Huang et al.[2] coupled the Jiles-Atherton equations with a lumped parameter vibratory model and included a phenomenological description of eddy current losses. Sarawate and Dapino[3] developed a uni-directionally coupled model where eddy currents in the magnetostrictive sample are described by solving the magnetic field diffusion equation. Some higher dimension models have also been proposed. Benbouzid[4] formulated a 2D bidirectionally coupled magnetostatic model where Terfenol-D constitutive behavior is incorporated using surface splines. Kannan and Dasgupta[5] formulated a 2D magnetostatic model with bi-directionally coupled magnetomechanical relations, current induced magnetic fields and electromagnetic body forces. Zhou et al.[6] developed a dynamic

Further author information: (Send correspondence to M.J.D)
S.C.: E-mail: chakrabarti.3@osu.edu, Telephone: 1-614-247-7480
M.J.D.: E-mail: dapino.1@osu.edu, Telephone: 1-614-688-3689

Behavior and Mechanics of Multifunctional Materials and Composites 2011,
Edited by Zoubeida Ounaies, Stefan S. Seelecke, Proc. of SPIE Vol. 7978, 79781C
 · doi: 10.1117/12.881159

finite element model of a unimorph actuator with one way magnetomechanical coupling. The one way coupled 3D model of Kim and Jung[7] describes force due to magnetostriction driving a coupled fluid-structural model for a sonar transducer. All these models take as input externally applied magnetic field, thus requiring additional description of the voltage-field relationship to relate system inputs and outputs. Aparicio and Sosa[8] describe a 3D, fully-coupled finite element model including dynamic effects but provide a very simple implementation for a magnetostrictive material with a single element. In order to describe transducer level input-output relationships for dynamic inputs, Evans and Dapino[9] presented a fully coupled dynamic model for 3D magnetostrictive transducers. The model simultaneously describes the effects of eddy currents, structural dynamics, and flux leakage on transducer performance. Due to the restriction of COMSOL Multiphysics being unable to handle vectorized functions, linear constitutive behavior is assumed.

This work aims at extending the framework by Evans and Dapino[9] to include nonlinear Galfenol behavior described using an efficient Discrete Energy Averaged Model (DEAM).[10] Nonlinear implementation is challenging due to the constitutive model inversion required for a vector magnetic potential based formulation and the inability of COMSOL Multiphysics to handle vectorized functions. For quasi-static operation, an efficient piecewise-linear solution strategy is proposed in section 4. This strategy is useful for obtaining accurate bias points. A linear dynamic simulation with piezomagnetic coefficients computed at the bias point describes the dynamic response of the system for moderate excitations. Finally, an implicit time integration scheme is discussed in section 6 to obtain the dynamic response of the system for large inputs. Comparison of these solutions to experiments conducted on a Galfenol unimorph actuator are presented in sections 5 and 7.

For magnetostatic problems, a partitioned solution approach is commonly followed in which magnetic and mechanical BVPs are solved separately, using the output of one as the input to the other.[4,11] For one way coupled models convergence is usually straightforward to achieve, but for bidirectional coupling a major iteration loop is required which can make convergence extremely slow. The methodology followed here is to formulate the coupled problem and solve for both physics simultaneously. This leads to faster convergence.

2. WEAK FORM EQUATIONS

The aim of the finite element model is to obtain the electromagnetic quantities, magnetic flux density ($\mathbf{B}$), magnetic field ($\mathbf{H}$), electric flux density ($\mathbf{D}$), electric field ($\mathbf{E}$), and the mechanical quantities, stress ($\mathbf{T}$) and strain ($\mathbf{S}$) in the system. The electrical and magnetic variables can be related using Maxwell's equations,

$$\nabla \times \mathbf{E} = -\frac{\partial \mathbf{B}}{\partial t}, \tag{1}$$

$$\nabla \cdot \mathbf{D} = \rho_q, \tag{2}$$

$$\nabla \times \mathbf{H} = \mathbf{J} + \frac{\partial \mathbf{D}}{\partial t}, \tag{3}$$

$$\nabla \cdot \mathbf{B} = 0, \tag{4}$$

while the mechanical variables can be described using Navier's equation,

$$\rho \frac{\partial^2 \mathbf{u}}{\partial t^2} + c \frac{\partial \mathbf{u}}{\partial t} = \nabla \cdot \mathbf{T} + \mathbf{f}_B. \tag{5}$$

Almost all formulations for electromechanical systems use a standard displacement-based formulation for the mechanical subsystem, meaning the solution variables are the mechanical displacements at the nodes of the model. Strain is obtained using the globally defined gradient operation on the displacement field, while stress is obtained using constitutive laws. For the electromagnetic subsystem different approaches are followed. Magnetostatic problems are often modeled using a scalar magnetic-potential-based approach[5] where the magnetic field is split up into a magnetization induced component, computed as the gradient of the scalar magnetic potential, and an externally imposed component entered as nodal force terms. The advantage of this procedure is that constitutive laws do not have to be inverted since most constitutive models take magnetic field as the input. The disadvantage of this formulation is that the current induced fields need to be specified manually but they are almost always unknown before solving the system. For the same reason, the formulation is restricted to quasi-static operating

conditions where eddy currents are absent. A vector magnetic-potential-based formulation[8,9] is more appropriate for dynamic modeling of magnetostrictive transducers since it allows direct inclusion of source current densities along with description of eddy current induced flux density changes. The vector magnetic potential $\mathbf{A}$ is defined as

$$\mathbf{B} = \nabla \times \mathbf{A}. \tag{6}$$

With this definition Gauss' Law (4) is identically satisfied. The second term in (3) models displacement current and can be neglected within the frequency bandwidth of operation of magnetostrictive transducers (< 30 kHz). Lorentz forces are neglected since the only component containing a significantly large current density in a magnetostrictive transducer is the drive coil which is structurally inactive. Finally, voltage gradients are neglected; the only source of electrical input is considered to be a source current density applied to the coil. Under these assumptions the only one of Maxwell's equations to be solved is (3), which is reduced to

$$\nabla \times \mathbf{H} = \mathbf{J}_s - \sigma \frac{\partial \mathbf{A}}{\partial t}. \tag{7}$$

The weak form equations can be derived using the method of weighted residuals as done by Evans et al.[9]

$$\int_{V_B} \mathbf{H} \cdot \delta\mathbf{B}\ dV + \int_{V_B} \sigma \frac{\partial \mathbf{A}}{\partial t} \cdot \delta\mathbf{A}\ dV = \int_{\partial V_B} (\mathbf{H} \times \mathbf{n}) \cdot \delta\mathbf{A}\ d\partial V + \int_{V_B} \mathbf{J}_s \cdot \delta\mathbf{A}\ dV, \tag{8}$$

$$\int_{V_u} \mathbf{T} \cdot \delta\mathbf{S}\ dV + \int_{V_u} \left(\rho \frac{\partial^2 \mathbf{u}}{\partial t^2} + c \frac{\partial \mathbf{u}}{\partial t} \right) \cdot \delta\mathbf{u}\ dV = \int_{\partial V_u} \mathbf{t} \cdot \delta\mathbf{u}\ d\partial V + \int_{V_u} \mathbf{f}_B \cdot \delta\mathbf{u}\ dV. \tag{9}$$

The solution variables for the problem are the mechanical displacement field ($\mathbf{u}$) and the vector magnetic potential ($\mathbf{A}$). The two equations (8) and (9) are decoupled in all domains except in Galfenol where the mechanical and magnetic states are coupled in a nonlinear manner. The first term in (8) and (9) suggests that the constitutive law should take ($\mathbf{B}$, $\mathbf{S}$) as inputs and calculate ($\mathbf{H}$, $\mathbf{T}$) as outputs. Almost all constitutive models work the other way around thus requiring model inversion. Since the models are nonlinear in nature, analytical inversion is in most cases impossible. Section 3 describes the constitutive law for Galfenol used in this work, while sections 4 and 6 discuss the inversion and incorporation of the constitutive law in the model.

3. DISCRETE ENERGY-AVERAGED MODEL (DEAM)

Incorporation of nonlinear constitutive behavior poses a significant challenge in the formulation of coupled finite element models for magnetostrictive systems. The most common method to describe magnetostrictive material behavior has been by obtaining polynomial fits to data. For example, Benbouzid et al.[12] used surface splines to fit experimental data while Kannan and Dasgupta[5] used constitutive relations in an incremental form with coefficients obtained from bicubic spline fits to measurements. Kim et al.[7] used 6^{th} order polynomials to fit the strain-field behavior with a different set of coefficients for each preload condition. The use of spline functions to fit measurements has the advantages of easy differentiability and implementation for 1D cases. However, the procedure becomes rather complex if complete 3D material behavior is required. This would require 3D measurements to be performed, and bulky splines with 9 components (3 for field and 6 for stress) to be fitted to those measurements. Graham et al.[11] implemented Galfenol constitutive behavior through look-up tables generated using the Armstrong model *a priori* for a large number of induction and stress values. Although the Armstrong model is capable of describing 3D Galfenol response, look-up tables were generated for 1D induction and stress inputs. As is the case with splines, extension to a full 3D version will add significant complexity because it will require generation of bulky tables with 9 inputs and 9 outputs. For these reasons, using an efficient constitutive law coded up as functions is beneficial for 3D boundary value problems.

The energy-averaged class of models describe macroscopic material response based on an energy weighted summation of contributions from domains aligned along different orientations. With fixed orientations (as in Armstrong's model[13]), good accuracy demands a large number of possible orientations to be considered which results in significant computational effort. To preserve accuracy along with computational efficiency, Evans and Dapino[10] restricted the number of possible orientations to six by considering only the directions which minimize a locally defined energy functional around each easy axis. The total free energy of a domain close to the k^{th} easy

axis $\mathbf{c}^k$ is formulated as the sum of local anisotropy energy G_A^k, magnetomechanical coupling energy G_C^k and the Zeeman energy G_Z^k as

$$G^k = \underbrace{\frac{1}{2}K^k|\mathbf{m}^k - \mathbf{c}^k|^2}_{G_A^k} - \underbrace{\mathbf{S}_m^k \cdot \mathbf{T}}_{G_C^k} - \underbrace{\mu_0 M_s \mathbf{m}^k \cdot \mathbf{H}}_{G_Z^k}. \tag{10}$$

Minimization of the energy functional and linearization of the unity norm constraint on the orientation vectors ($\mathbf{m}^k \cdot \mathbf{m}^k = 1 \approx \mathbf{c}^k \cdot \mathbf{m}^k = 1$) yields the following analytical expression for the k^{th} local minimum

$$\mathbf{m}^k = \left(\mathbf{K}^k\right)^{-1} \left[\mathbf{B}^k + \frac{1 - \mathbf{c}^k \cdot \left(\mathbf{K}^k\right)^{-1} \mathbf{B}^k}{\mathbf{c}^k \cdot \left(\mathbf{K}^k\right)^{-1} \mathbf{c}^k} \mathbf{c}^k\right], \tag{11}$$

where the magnetic stiffness matrix $\mathbf{K}^k$ and force vector $\mathbf{B}^k$ are

$$\mathbf{K}^k = \begin{bmatrix} K^k - 3\lambda_{100}T_1 & -3\lambda_{111}T_4 & -3\lambda_{111}T_6 \\ -3\lambda_{111}T_4 & K^k - 3\lambda_{100}T_2 & -3\lambda_{111}T_5 \\ -3\lambda_{111}T_6 & -3\lambda_{111}T_5 & K^k - 3\lambda_{100}T_3 \end{bmatrix}, \tag{12}$$

$$\mathbf{B}^k = \begin{bmatrix} c_1^k K^k + \mu_0 M_s H_1 & c_2^k K^k + \mu_0 M_s H_2 & c_3^k K^k + \mu_0 M_s H_2 \end{bmatrix}^{\mathrm{T}}. \tag{13}$$

The anhysteretic volume fractions are calculated using Boltzmann-type averaging,

$$\xi_{an}^k = \frac{\exp\left(-G^k/\Omega\right)}{\sum_{j=1}^{r} \exp\left(-G^j/\Omega\right)}, \tag{14}$$

where Ω is an averaging factor. Macroscopic anhysteretic material behavior is obtained by summing the individual contributions of each domain weighted by its corresponding volume fraction. The DEAM is extremely efficient since it includes energy weighted summation of only six terms and analytical expressions to calculate the minima. Moreover it can be analytically differentiated to obtain the matrix of material coefficients. This property is particularly useful for formulating a piecewise-linear solution procedure described in section 4, as well as in the numerical inversion process for the nonlinear dynamic solution discussed in section 6.

4. PIECEWISE-LINEAR SOLUTION PROCEDURE

Under quasi-static conditions, the weak form equations (8) and (9) can be written in incremental form as

$$\int_{V_B} \Delta\mathbf{H} \cdot \delta\Delta\mathbf{B}\, dV \int_{\partial V_B} (\Delta\mathbf{H} \times n) \cdot \delta\Delta\mathbf{A}\, d\partial V + \int_{V_B} \Delta\mathbf{J}_s \cdot \delta\Delta\mathbf{A}\, dV, \tag{15}$$

$$\int_{V_u} \Delta\mathbf{T} \cdot \delta\Delta\mathbf{S}\, dV = \int_{\partial V_u} \Delta\mathbf{t} \cdot \delta\Delta\mathbf{u}\, d\partial V + \int_{V_u} \Delta\mathbf{f}_B \cdot \delta\Delta\mathbf{u}\, dV, \tag{16}$$

where $\Delta\mathbf{H}$ and $\Delta\mathbf{T}$ must be computed as a function of $\Delta\mathbf{B}$ and $\Delta\mathbf{S}$. For some field $\mathbf{H}_0$ and stress $\mathbf{T}_0$, the DEAM however computes $\mathbf{B}$ and $\mathbf{S}$ along with the matrix of derivatives $\mathcal{J}$ given by

$$\mathcal{J} = \begin{bmatrix} \boldsymbol{\mu} = \frac{\partial \mathbf{B}}{\partial \mathbf{H}}(\mathbf{H}_0, \mathbf{T}_0) & \mathbf{d} = \frac{\partial \mathbf{B}}{\partial \mathbf{T}}(\mathbf{H}_0, \mathbf{T}_0) \\ \mathbf{d}^T = \frac{\partial \mathbf{S}}{\partial \mathbf{H}}(\mathbf{H}_0, \mathbf{T}_0) & \mathbf{s} = \frac{\partial \mathbf{S}}{\partial \mathbf{T}}(\mathbf{H}_0, \mathbf{T}_0) \end{bmatrix}. \tag{17}$$

For small deviations about $\mathbf{H}_0$ and $\mathbf{T}_0$, the constitutive law can be formulated in incremental form as

$$\begin{bmatrix} \Delta\mathbf{H} \\ \Delta\mathbf{T} \end{bmatrix} = \underbrace{\begin{bmatrix} \boldsymbol{\mu}^i & -\mathbf{a} \\ -\mathbf{a}^{\mathrm{T}} & \mathbf{c} \end{bmatrix}}_{\mathcal{J}^{-1}} \begin{bmatrix} \Delta\mathbf{B} \\ \Delta\mathbf{S} \end{bmatrix}. \tag{18}$$

Since the computed piezomagnetic coefficients are dependent on stress and field, which have a spatial variation, the coefficients are also spatially variant. To preserve this inhomogeneity, the coefficients are declared as interpolated data functions of spatial coordinates. Each piezomagnetic coefficient is a separate function and when called, COMSOL searches in the data file for their values corresponding to that location or interpolates between nearby points if that location is not present in the file. A total of 33 coefficients is used:

$$\boldsymbol{\mu}^i = \begin{bmatrix} \mu^i_{11} & \mu^i_{12} & \mu^i_{13} \\ \mu^i_{12} & \mu^i_{22} & \mu^i_{23} \\ \mu^i_{13} & \mu^i_{23} & \mu^i_{33} \end{bmatrix}, \ \mathbf{a} = \begin{bmatrix} a_{11} & a_{12} & a_{13} & a_{14} & a_{15} & a_{16} \\ a_{21} & a_{22} & a_{23} & a_{24} & a_{25} & a_{26} \\ a_{31} & a_{32} & a_{33} & a_{34} & a_{35} & a_{36} \end{bmatrix}, \ \mathbf{c} = \begin{bmatrix} c_{11} & c_{12} & c_{13} & 0 & 0 & 0 \\ c_{12} & c_{22} & c_{23} & 0 & 0 & 0 \\ c_{13} & c_{23} & c_{33} & 0 & 0 & 0 \\ 0 & 0 & 0 & c_{44} & 0 & 0 \\ 0 & 0 & 0 & 0 & c_{55} & 0 \\ 0 & 0 & 0 & 0 & 0 & c_{66} \end{bmatrix}. \quad (19)$$

Ideally, the coefficients must be evaluated at all the integration points present in the Galfenol subdomain during the assembly process. In a 3D model several thousand integration points are present. Evaluation, inversion and storage of the Jacobian at every integration point is both computationally expensive and memory intensive. Assuming that the spatial variation in field and stress is not extremely drastic, the coefficients are calculated only at selected locations and evaluated at the remaining points through interpolation.

Figure 1 shows the overall piecewise linear solution procedure. The process is fast as it does not involve iteration loops or convergence checks. Consequently, the solution has a drift error which becomes larger with increasing step size. Thus using a sufficiently small step size is necessary to ensure an accurate solution. The piecewise linear model is useful for two purposes. First, to obtain a measure of quasi-static system performance and secondly to generate accurate bias points which preserve the spatial inhomogeneity in the distribution of field and stress in Galfenol, and hence, the piezomagnetic coefficients. A measure of dynamic response for moderate inputs about the bias point can be obtained using these piezomagnetic coefficients.

5. PIECEWISE LINEAR MODEL RESULTS

The finite element framework described in the previous sections is validated using a Galfenol unimorph actuator shown in Figure 2(a). The actuator consists of a composite beam having a Galfenol layer bonded to a brass substrate, a drive coil, and steel flux return components. The system is excited by applying a voltage input to the coil and the vertical tip deflection of the beam is measured with a laser displacement sensor.

Piecewise-linear quasi-static solution

Quasi-static measurements are collected by cycling the voltage at 0.1 Hz. In the model, input is applied in the form of small increments to the coil source current density and solution is obtained using the piecewise-linear approach outlined in Figure 1. Beam tip deflection is obtained by integrating the vertical displacement component over the free edge of the Galfenol layer. The simulation describes the nonlinearity in the beam deflection response (see Figure 3) accurately. The voltage current curve is a straight line whose slope is the dc resistance of the coil.

Linear dynamic simulation about bias point

Harmonic response of the beam is obtained by applying a bias voltage of 7 V and subsequently applying sinusoidal voltage inputs at distinct frequencies. The amplitude of the sinusoidal voltage signal is increased with increasing frequency to keep the current levels comparable so as to obtain good measurable deflections at the beam tip. Figure 4 shows the results of the linear dynamic simulation at 10 Hz and 100 Hz. At 10 Hz, the model slightly over-predicts the tip-deflection because of its linear nature. However, as the frequency increases the inertia and damping forces dominate over the material nonlinearity and smooths out the overall system response which results in better accuracy.

The linear dynamic solution gives a fairly accurate description of the dynamic performance of the transducer for moderate inputs about a bias point. However, since Galfenol exhibits moderate magnetostriction, most applications require the transducer to be operated with larger inputs utilizing the full nonlinear strain of Galfenol. To obtain such description a nonlinear dynamic solution procedure is formulated as described in the next section.

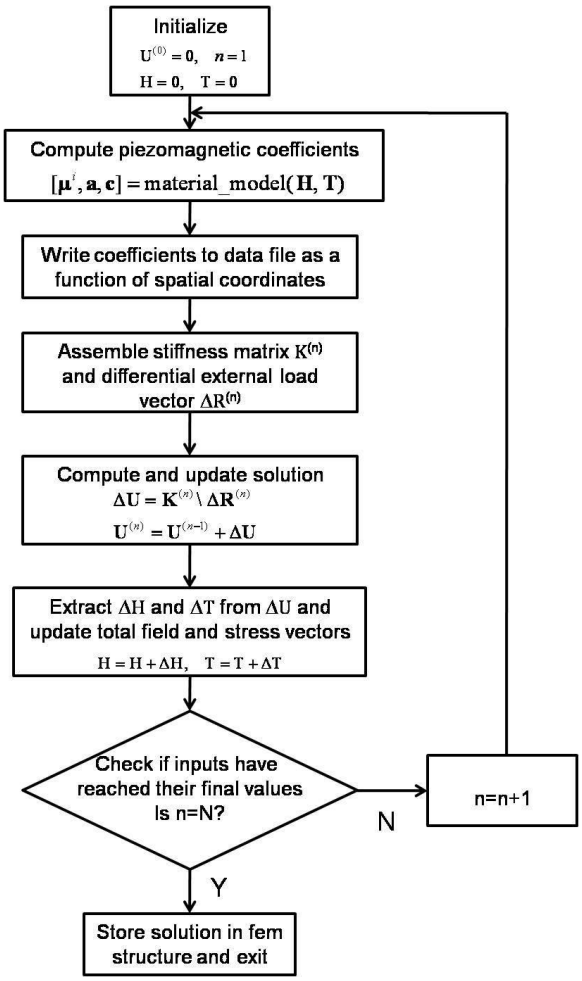

Figure 1. Flowchart of the piecewise-linear solution process.

6. NONLINEAR DYNAMIC SOLUTION PROCEDURE

Solution of nonlinear dynamic systems is a particularly challenging task as even unconditionally stable time integration schemes for linear systems may become unstable. The governing equations for the finite element system described in section 2 can be written as

$$\mathbf{M}\ddot{\mathbf{U}} + \mathbf{D}\dot{\mathbf{U}} = \mathbf{R}(t) - \mathbf{F}(\mathbf{U}, t), \tag{20}$$

where the mass matrix $\mathbf{M}$, damping matrix $\mathbf{D}$, and state vector $\mathbf{U}$ are of the form

$$\mathbf{M} = \begin{bmatrix} \mathbf{0} & \mathbf{0} \\ \mathbf{0} & \mathbf{M}^u \end{bmatrix}, \quad \mathbf{D} = \begin{bmatrix} \mathbf{D}^A & \mathbf{0} \\ \mathbf{0} & \mathbf{D}^u \end{bmatrix}, \quad \mathbf{U} = \begin{pmatrix} \mathbf{Q}^A \\ \mathbf{Q}^u \end{pmatrix}. \tag{21}$$

The vector of externally applied forces $\mathbf{R}(t)$ includes contributions from the coil source current density and/or traction on certain boundaries; $\mathbf{F}(\mathbf{U}, t)$ is the internal nodal force vector whose derivative with respect to the state vector $\mathbf{U}$ yields the stiffness matrix. Since $\mathbf{F}$ contains contributions from element field and stress which are nonlinearly dependent on $\mathbf{U}$, the stiffness matrix $\mathbf{K}$ is also state dependent. Evaluation of $\mathbf{F}$ and $\mathbf{K}$ are the most time consuming operations in the solution process.

Bathe[14] suggested various time-integration schemes for nonlinear structural problems of similar form. Explicit methods are ruled out since the mass matrix is singular. An implicit scheme based on the trapezoidal rule is

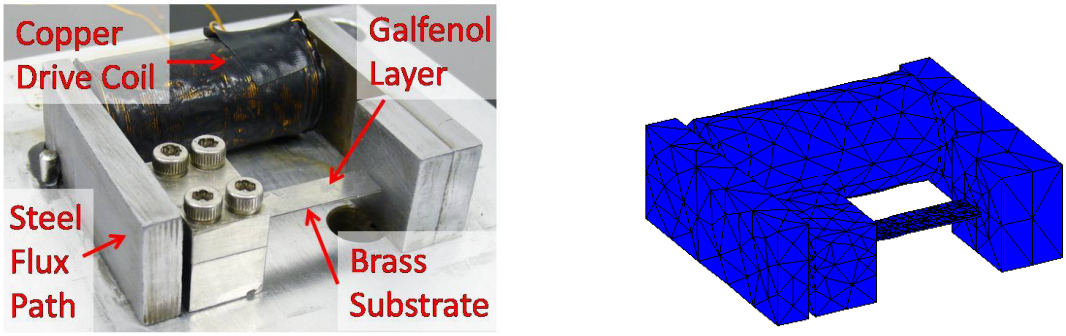

(a) (b)

Figure 2. The Galfenol unimorph actuator used for model validation, (a) geometry, (b) mesh.

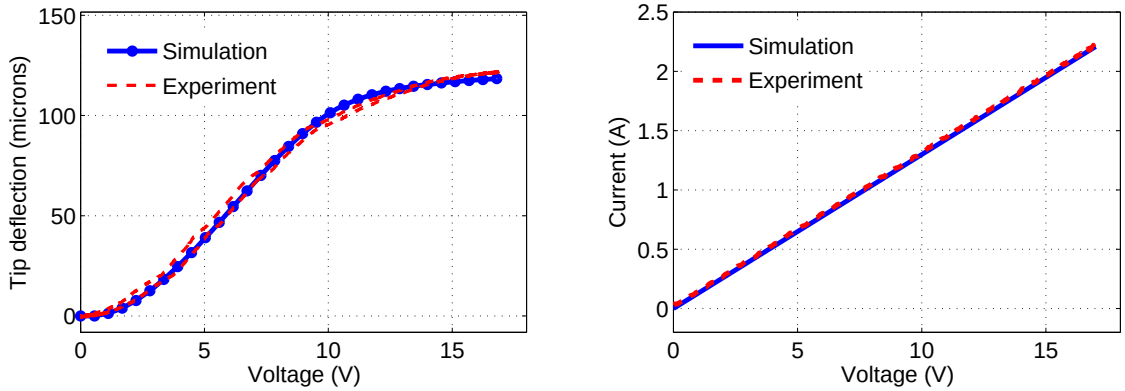

(a) (b)

Figure 3. Quasi-static model results, (a) voltage-deflection, (b) voltage-current.

implemented, combined with equilibrium iterations. At the k^{th} iteration the system equations can be written as

$$\mathbf{M}^{t+\Delta t}\ddot{\mathbf{U}}^{(k)} + \mathbf{D}^{t+\Delta t}\dot{\mathbf{U}}^{(k)} + {}^{t+\Delta t}\mathbf{K}^{(k-1)}\Delta\mathbf{U}^{(k)} = {}^{t+\Delta t}\mathbf{R} - {}^{t+\Delta t}\mathbf{F}^{(k-1)}, \tag{22}$$

$${}^{t+\Delta t}\mathbf{U}^{(k)} = {}^{t+\Delta t}\mathbf{U}^{(k-1)} + \Delta\mathbf{U}^{(k)}. \tag{23}$$

According to the trapezoidal rule of time integration, the following assumptions are used;

$${}^{t+\Delta t}\mathbf{U} = {}^{t}\mathbf{U} + \frac{\Delta t}{2}\left({}^{t}\dot{\mathbf{U}} + {}^{t+\Delta t}\dot{\mathbf{U}}\right), \tag{24}$$

$${}^{t+\Delta t}\dot{\mathbf{U}} = {}^{t}\dot{\mathbf{U}} + \frac{\Delta t}{2}\left({}^{t}\ddot{\mathbf{U}} + {}^{t+\Delta t}\ddot{\mathbf{U}}\right). \tag{25}$$

The vectors $\ddot{\mathbf{U}}^{(k)}$ and $\dot{\mathbf{U}}^{(k)}$ can be written using (23) to (25) as

$${}^{t+\Delta t}\ddot{\mathbf{U}}^{(k)} = \frac{4}{\Delta t^2}\left({}^{t+\Delta t}\mathbf{U}^{(k-1)} - {}^{t}\mathbf{U} + \Delta\mathbf{U}^{(k)}\right) - \frac{4}{\Delta t}{}^{t}\dot{\mathbf{U}} - {}^{t}\ddot{\mathbf{U}}, \tag{26}$$

$${}^{t+\Delta t}\dot{\mathbf{U}}^{(k)} = \frac{2}{\Delta t}\left({}^{t+\Delta t}\mathbf{U}^{(k-1)} - {}^{t}\mathbf{U} + \Delta\mathbf{U}^{(k)}\right) - {}^{t}\dot{\mathbf{U}}. \tag{27}$$

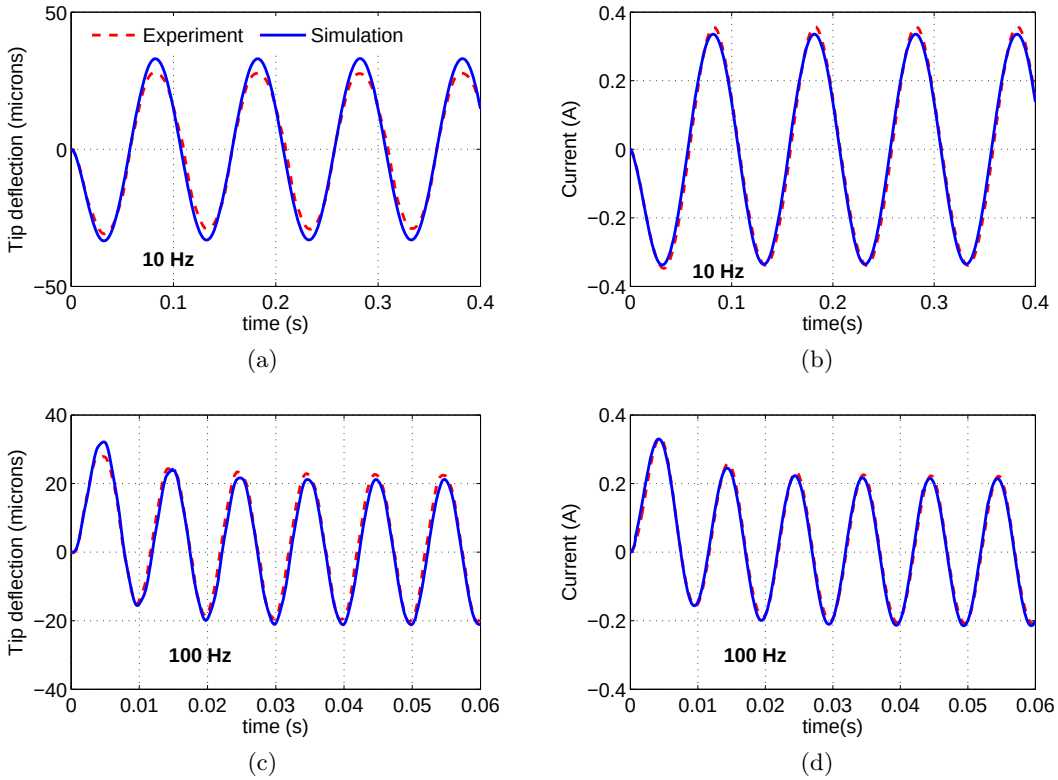

Figure 4. Experimental and model predicted results for beam tip deflection and current at different frequencies.

Substitution in (22) yields the equation of motion for the system;

$$\left[{}^{t+\Delta t}\mathbf{K}^{(k-1)} + \frac{4\mathbf{M}}{\Delta t^2} + \frac{2\mathbf{D}}{\Delta t}\right]\Delta\mathbf{U}^{(k)} = {}^{t+\Delta t}\mathbf{R} - \mathbf{M}\left[\frac{4}{\Delta t^2}\left({}^{t+\Delta t}\mathbf{U}^{(k-1)} - {}^{t}\mathbf{U}\right) - \frac{4}{\Delta t}{}^{t}\dot{\mathbf{U}} - {}^{t}\ddot{\mathbf{U}}\right] - \mathbf{D}\left[\frac{2}{\Delta t}\left({}^{t+\Delta t}\mathbf{U}^{(k-1)} - {}^{t}\mathbf{U}\right) - {}^{t}\dot{\mathbf{U}}\right] - {}^{t+\Delta t}\mathbf{F}^{(k-1)}. \tag{28}$$

The starting values for the internal force and state vector are considered to be same as the corresponding final values of the previous time step;

$${}^{t+\Delta t}\mathbf{F}^{(0)} = {}^{t}\mathbf{F}, \quad {}^{t+\Delta t}\mathbf{U}^{(0)} = {}^{t}\mathbf{U}. \tag{29}$$

The convergence criteria used in this work are based on energy and norm of the out-of-balance load vector.[14] Mathematically they can be written as

$$\frac{\|{}^{t+\Delta t}\mathbf{R} - {}^{t+\Delta t}\mathbf{F}^{(k-1)} - \mathbf{M}\,{}^{t+\Delta t}\ddot{\mathbf{U}}^{(k-1)} - \mathbf{D}\,{}^{t+\Delta t}\dot{\mathbf{U}}^{(k-1)}\|}{RNORM} \leq RTOL, \tag{30}$$

$$\frac{\Delta\mathbf{U}^{(k)} \cdot \left({}^{t+\Delta t}\mathbf{R} - {}^{t+\Delta t}\mathbf{F}^{(k-1)} - \mathbf{M}\,{}^{t+\Delta t}\ddot{\mathbf{U}}^{(k-1)} - \mathbf{D}\,{}^{t+\Delta t}\dot{\mathbf{U}}^{(k-1)}\right)}{\Delta\mathbf{U}^{(1)} \cdot \left({}^{t+\Delta t}\mathbf{R} - {}^{t}\mathbf{F} - \mathbf{M}\,{}^{t}\ddot{\mathbf{U}} - \mathbf{D}\,{}^{t}\dot{\mathbf{U}}\right)} \leq ETOL. \tag{31}$$

The mass and damping matrix are state-independent and hence are assembled only once for the entire simulation. The internal nodal force vector $\mathbf{F}$ and the tangential stiffness matrix $\mathbf{K}$ are assembled in every iteration as they are state-dependent. Evaluation of $\mathbf{F}$ requires computation of the total stress and field for a given flux density and strain distribution, for which the DEAM needs to be inverted. This is done using the Quasi-Newton SR1 formula which updates the Jacobian inverse directly, eliminating the need for matrix inversion within the iteration loop.

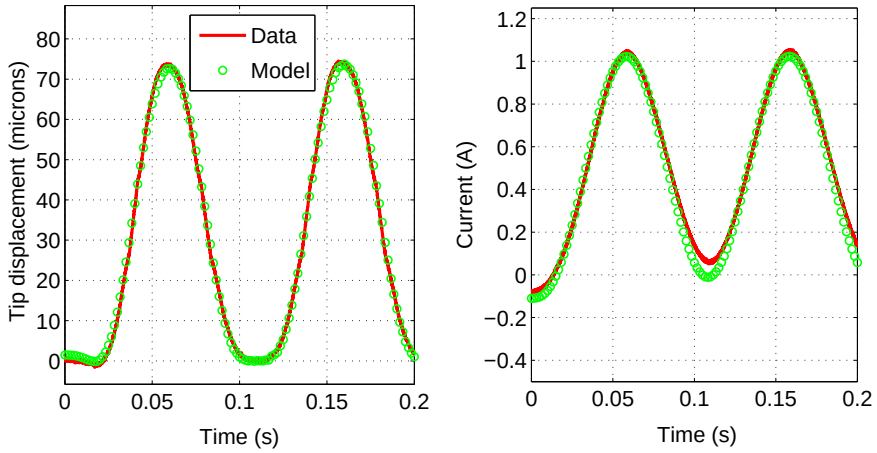

Figure 5. Actuator response to harmonic excitation at 10 Hz.

The computed Jacobian inverse in the final iteration of the inversion process is used for the assembly of the global stiffness matrix. Thus, the material model is inverted only once for every integration point and the values of the 3 field components, 6 stress components and 81 terms of the material Jacobian inverse matrix are stored in a global data structure in MATLAB. Since COMSOL cannot take vector-valued inputs from MATLAB functions, it calls the same function multiple times to assemble the matrices. The material model is coded up such that it is executed only once for a particular set of input values and returns directly from the stored data structure for the remaining number of times.

7. NONLINEAR DYNAMIC MODEL RESULTS

The same Galfenol unimorph actuator (Figure 2) is used to validate the nonlinear dynamic solution procedure. Harmonic excitations ranging from 10 Hz to 200 Hz are applied to the system in the form $V(t) = -V_{bias} + V_0(1 - cos(2\pi ft))$. The finite element model is run only for the time duration of the first few cycles. In order to obtain appreciable displacement response from the beam at higher frequencies a negative bias voltage (V_{bias}) is applied first before applying the harmonic signal. This ensures that the effective bias point of the cyclic signal is in the burst region. In the model the bias point is obtained in a similar fashion by applying the bias voltage smoothed using a tanh function for ease of convergence. Figures 5 - 8 show the transient response of the transducer for harmonic inputs at 10, 50, 100, and 200 Hz. The modeled responses show good correlation with the experiments particularly for the tip deflection response. An interesting outcome of nonlinear Galfenol behavior can be seen where the quadratic nonlinearity of the magnetostrictive strain at zero field causes frequency doubling in the tip deflection response. An interesting observation is the relationship between current in the coil and magnetic field in Galfenol which is often approximated by a linear relationship. Figure 9 shows that there is some hysteresis in the current-field loop even at 10 Hz. At 50 Hz the hysteresis is considerably larger. This implies that a linear current-field assumption may introduce significant errors in predicting the phase of the output, particularly at higher frequencies.

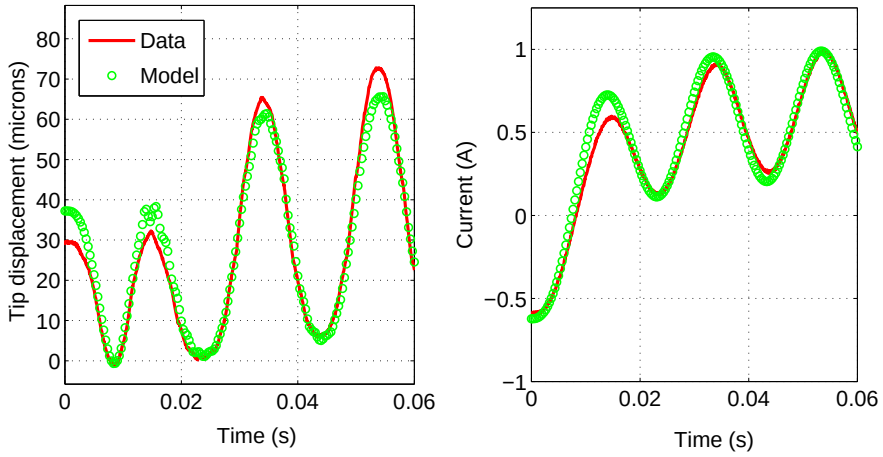

Figure 6. Actuator response to harmonic excitation at 50 Hz.

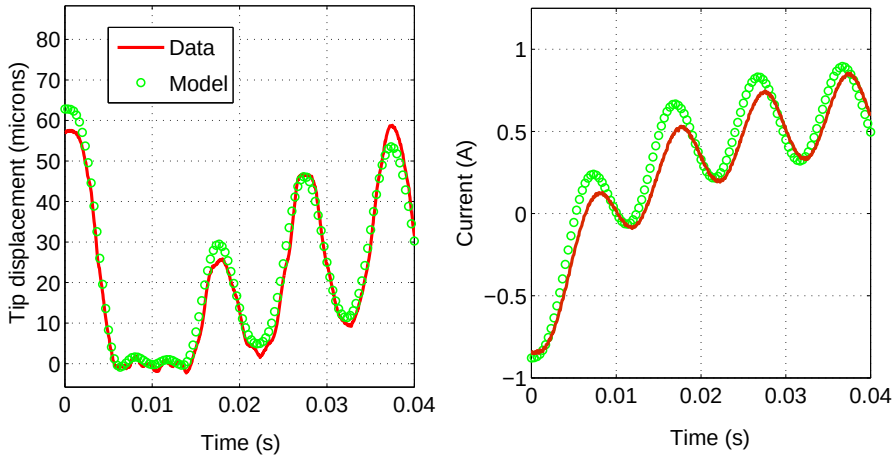

Figure 7. Actuator response to harmonic excitation at 100 Hz.

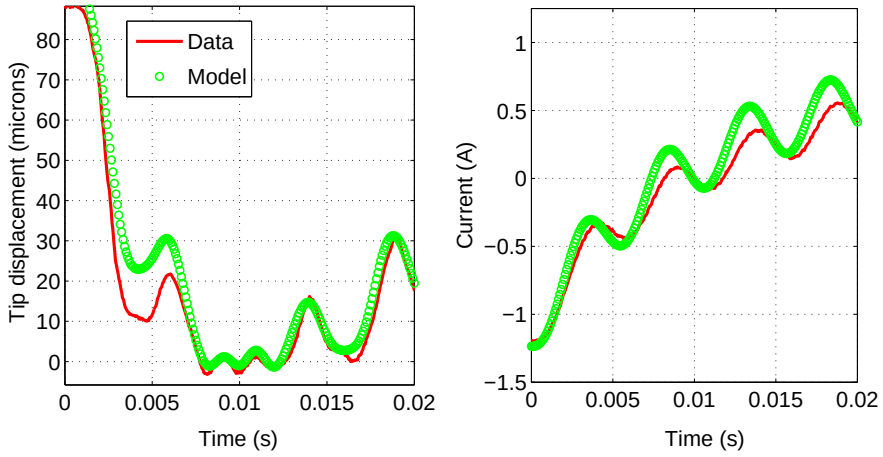

Figure 8. Actuator response to harmonic excitation at 200 Hz.

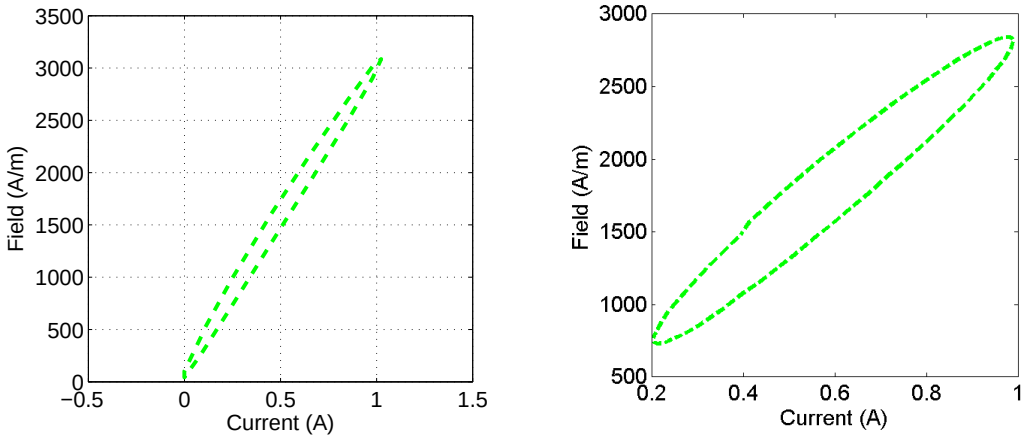

(a) (b)

Figure 9. Modeled relationship between drive current in the coil and average axial field in the Galfenol beam (a) 10 Hz and (b) 50 Hz.

8. CONCLUDING REMARKS

The paper presented a finite element framework for modeling 3D Galfenol transducers driven over nonlinear regimes with dynamic inputs. Weak form equations derived from Maxwell's equations for electromagnetics and Navier's equation for mechanical systems are coded into COMSOL (a commercial finite element software), which is used for meshing, global assembly of matrices and post-processing. Galfenol constitutive behavior is incorporated using a nonlinear energy-averaged model. A piecewise-linear solution strategy is found to be useful for obtaining quasi-static system response and accurate bias point determination. A linear dynamic simulation with piezomagnetic coefficients computed at the bias point provides an accurate description of dynamic performance for moderate inputs. An implicit time integration scheme based on the trapezoidal rule yields the dynamic response of the system for large-scale inputs. As is required for any vector magnetic-potential-based formulation, the constitutive law is inverted numerically using Quasi-Newton iterations. Efficiency is maintained by coding up the material model such that executing the inversion routine only once calculates the 6 components of stress, 3 components of field and 81 components of the Jacobian inverse. The inability of COMSOL to accept vector valued inputs from MATLAB functions is overcome by using a global data structure. The model is validated using a Galfenol unimorph actuator. Results show that the modeled responses compare well with experiments and describe the key features which occur due to nonlinear behavior of Galfenol. The framework also brings out some shortcomings of a linear current-field relationship assumed in models with reduced order coupling.

ACKNOWLEDGMENTS

Support for this research is provided by the Office of Naval Research, MURI grant # N000140610530.

REFERENCES

[1] Dapino, M., Smith, R., and Flatau, A., "Structural magnetic strain model for magnetostrictive transducers," *IEEE Transactions on Magnetics* **36**, 545–556 (May 2000).

[2] Huang, W., Wang, B., Cao, S., Sun, Y., Weng, L., and Chen, H., "Dynamic strain model with eddy current effects for giant magnetostrictive transducer," *IEEE Transactions on Magnetics* **43**, 1381–1384 (April 2007).

[3] Sarawate, N. and Dapino, M., "A dynamic actuation model for magnetostrictive materials," *Smart Materials and Structures* **17**, 065013 (2008).

[4] Benbouzid, M., Beguenane, R., Reyne, G., and Meunier, G., "Finite element modeling of Terfenol-D magneto-mechanical coupling: application to a direct micro-stepping rotary motor," (1997).

[5] Kannan, K. and Dasgupta, A., "A nonlinear Galerkin finite-element theory for modeling magnetostrictive smart structures," *Smart Materials and Structures* **6**, 341–350 (1997).
[6] Zhou, H. and Zhou, Y., "Vibration suppression of laminated composite beams using actuators of giant magnetostrictive materials," *Smart materials and structures* **16**, 198–206 (2007).
[7] Kim, J. and Jung, E., "Finite element analysis for acoustic characteristics of a magnetostrictive transducer," *Smart Materials and Structures* **14**, 1273–1280 (2005).
[8] Pérez-Aparicio, J. and Sosa, H., "A continuum three-dimensional, fully coupled, dynamic, non-linear finite element formulation for magnetostrictive materials," *Smart Materials and Structures* **13**, 493–502 (2004).
[9] Evans, P. and Dapino, M., "Dynamic Model for 3-D Magnetostrictive Transducers," *Magnetics, IEEE Transactions on* **47**(1), 221–230 (2011).
[10] Evans, P. G. and Dapino, M. J., "Efficient magnetic hysteresis model for field and stress application in magnetostrictive galfenol," *Journal of Applied Physics* **107**(6), 063906 (2010).
[11] Graham, F., Mudivarthi, C., Datta, S., and Flatau, A., "Modeling of a Galfenol transducer using the bidirectionally coupled magnetoelastic model," *Smart Materials and Structures* **18**, 104013 (2009).
[12] Benbouzid, M., Reyne, G., Meunier, G., Kvarnsjo, L., and Engdahl, G., "Dynamic modelling of giant magnetostriction in Terfenol-D rods by the finite element method," *Magnetics, IEEE Transactions on* **31**(3), 1821–1824 (1995).
[13] Armstrong, W., "Magnetization and magnetostriction processes in $\mathrm{tb}_0.27 - 0.30\mathrm{dy}_0.73 - 0.70\mathrm{fe}_1.9 - 2.0$," *Journal of Applied Physics* **81**(5), 23217–2326 (1997).
[14] Bathe, K., [*Finite Element Procedures*], Prentice Hall, Upper Saddle River, New Jersey 07458 (1996).